Available online at www.sciencedirect.com
SCIENCE DIRECT®
Polymer 44 (2003) 4689–4698
polymer
www.elsevier.com/locate/polymer

Miscibility and phase behavior in thermosetting blends of polybenzoxazine and poly(ethylene oxide)☆

Han Lü, Sixun Zheng*

Department of Polymer Science and Engineering, Shanghai Jiao Tong University, 800 Dongchuan Road, Shanghai 200240, People's Republic of China

Received 21 January 2003; received in revised form 28 April 2003; accepted 13 May 2003

Abstract

Thermosetting polymer blends composed of polybenzoxazine (PBA-a) and poly(ethylene oxide) (PEO) were prepared via in situ curing reaction of benzoxazine (BA-a) in the presence of PEO, which started from the initially homogeneous mixtures of BA-a and PEO. Before curing, the BA-a/PEO blends displayed the single and composition-dependant glass transition temperatures (T_g's) in the entire blend composition, and the equilibrium melting point depression was also observed in the blends. It is judged that the BA-a/PEO blends are completely miscible. The miscibility was mainly ascribed to the contribution of entropy to mixing free energy since the molecular weight of BA-a is rather low. However, phase separation occurred after curing reaction at the elevated temperature, which was confirmed by differential scanning calorimetry (DSC) and scanning electronic microscopy (SEM). It was expected that the PBA-a/PEO blends would be miscible since PBA-a possesses a great number of phenolic hydroxyls in the molecular backbone, which are potential to form the intermolecular hydrogen bonding interactions with oxygen atoms of PEO and thus would fulfill the miscibility of the blends. To interpret the experimental results, we investigated the variable temperature Fourier transform infrared spectroscopy (FTIR) of the blends via model compound. The FTIR results indicate that the phenolic hydroxyl groups could not form the efficient intermolecular hydrogen bonding interactions at the elevated temperatures (e.g. the curing temperatures), i.e. the phenolic hydroxyl groups existed mainly in the non-associated form in the system. Therefore, the decrease of the mixing entropy still dominates the phase behavior of thermosetting blends at the elevated temperature.

Keywords: Polybenzoxazine; Poly(ethylene oxide); Thermosetting blends

1. Introduction

Thermosetting polymer blends have provoked considerable interests during the last decades [1–23]. Thermodynamically, the formation of crosslinked structure is unfavorable for the entropic contribution to the mixing free energy due to the molecular weight of infinity for crosslinked components. As a consequence, phase separation occurs owing to the endothermic enthalpy of mixing. In fact, most of the thermosetting polymer blends found hitherto are immiscible unless there exist the favorable intermolecular specific interactions (e.g. hydrogen bonding); the intermolecular specific interactions have been taken as the driving force for miscibility in some thermosetting polymer blends [21–23]. It is the formation of phase-separated morphologies that endows the improved toughness of thermosetting polymers. In addition to the governing factor of thermodynamics, phase behavior of thermosetting blends could be affected by the kinetics involved with the curing process of thermosetting polymer blends, e.g. polymerization and phase separation. It is reported [24] that the competitive kinetics between polymerization and phase separation significantly affected the resulting morphology of the thermosetting polymer blends of epoxy resin and poly(hydroxyether of bisphenol A). It is important to investigate the impact of the curing process on phase behavior for understanding the relationship between the structure and properties of the thermosetting polymer blends.

Polybenzoxazine (PBA-a) is a class of attractive phenolic- resins and it can be used as the matrices of

☆ The abstract has been presented in the 19th polymer processing society annual meeting, Melbourne, Australia, July 2003.

* Corresponding author. Tel.: +86-21-54743278; fax: +86-21-54741297.
E-mail address: szheng@sjtu.edu.cn (S. Zheng).

0032-3861/03/$ - see front matter © 2003 Elsevier Science Ltd. All rights reserved.
doi:10.1016/S0032-3861(03)00401-4

high-performance composites because of its superior mechanical properties and high-temperature stability. PBA-a possesses excellent processability through a very wide range of molecular design flexibility [25–27]. The potential applications of PBA-a motivate to prepare their thermosetting blends with improved properties [28–30,39]. Recently, Ishida et al.. [28] investigated that the thermal properties and dynamic mechanical properties in the blends of PBA-a and poly(ε-caprolactone) (PCL). It is recognized that there are the intermolecular hydrogen bonding interactions in this blend system via the phenolic hydroxyls of PBA-a and carbonyls of PCL [29].

In this contribution, we present our investigation of the thermosetting polymer blends composed of PBA-a and poly(ethylene oxide) (PEO), a semi-crystalline polymer. In terms of the chemical structures of the blend pairs, it could be expected that there are the intermolecular hydrogen bonding interactions between phenolic hydroxyls of PBA-a and ether oxygen atoms of PEO, which could promote the miscibility of the resulting blends. Nonetheless, the presence of the functional groups unnecessarily purports the formation of the intermolecular specific interactions since the curing process at elevated temperature could significantly reduce the efficient intermolecular specific interactions. In addition, the steric shielding and accessibility of functional groups could reduce and even prohibit the intermolecular hydrogen bonding interactions due to the formation of the crosslinked networks. The above factors will effectively reduce the contribution of mixing enthalpy (ΔH_m) to the free energy of mixing (ΔG_m) vis-à-vis analogous low-molecular-weight analogues [31–38]. The goal of this work is to evaluate the role of intermolecular hydrogen bonding interactions in the formation of resulting morphology of the blends. The miscibility, phase behavior of the blends after and before curing reaction was addressed on the basis of thermal analysis (DSC) and scanning electronic microscopy (SEM).

2. Experimental

2.1. Materials and preparation of samples

PEO was purchased from Shanghai Reagents Co., China; it has a quoted molecular weights of $M_n = 20,000$. Benzoxazine (BA-a) monomer was synthesized from bisphenol A, paraformaldehyde and aniline via Mannich condensation as described elsewhere [25] (Scheme 1).

Typically, to a 500 ml three-necked round flask equipped with a reflux condenser and a mechanical stirring bar 80 ml of 1,4-dioxane, 32.4 ml of formaline (40%) (12 g, 0.4 mol), 18.8 g (0.2 mol) of aniline were charged, keeping the temperature below 10 °C, and the mixture was stirred for 10 min before 23.4 g (0.1 mol) of bisphenol A was added to the solution. The temperature was then raised and the reactive system was refluxed for 16 additional hours with

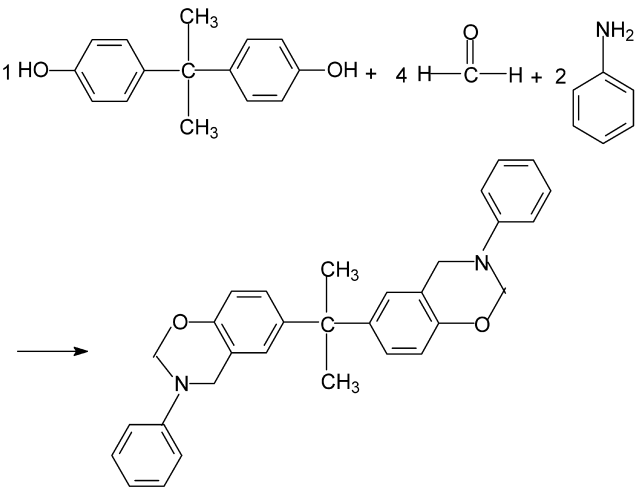

Scheme 1.

continuously stirring. The reactive system was cooled down to the room temperature and 40 ml of ethyl ether was added to system and the white crystals of BA-a were separated out. The products were dissolved with chloroform and re-crystallization with ethyl ether, and the procedure was repeated three times. The BA-a was dried in a vacuum oven before use. All the chemicals are of reagent grade, obtained from Shanghai Reagents Co. China and used as received.

The blends of BA-a with PEO were prepared by casting from chloroform solution at room temperature. The residual solvent was removed by drying in a vacuum oven at 60 °C for 2 days. To prepare PBA-a/PEO blends, BA-a and PEO were mixed at the temperature above the melting point of PEO (100 °C) for sufficiently long time until the clear, homogeneous mixtures were obtained. The blends were allowed to cure in aluminum foils. The curing schedule was set as 180 °C for 4 h to attain a complete curing reaction.

2.2. Measurement

Differential scanning calorimetry (*DSC*). The calorimetric measurement was performed on a Perkin–Elmer Pyris 1 differential scanning calorimeter in a dry nitrogen atmosphere. The instrument was calibrated with standard Indium. To remove the thermal history of the samples, a thermal pretreatment was used. All samples (about 10 mg in weight) were heated up to the elevated temperatures (100 °C for BA-a/PEO blends and 180 °C for PBA-a/PEO blends) and held for 3 min, and then quenched to −70 °C. The DSC thermograms were recorded at a heating rate of 20 °C/min. The glass transition temperatures were taken as the midpoint of the capacity transition. The crystallization temperatures (T_c) and the melting temperatures (T_m) were taken as the temperatures at maximum and the minimum of both endothermic and exothermic peaks, respectively.

Determination of equilibrium melting points. The equilibrium melting points of the BA-a/PEO blends were measured by polarized optical microscopy (POM) (Leica

DMP system) equipped with a hot stage (Linkam TH960, Linkam Scientific Instruments, Ltd) with a precision of ±0.1 °C. The blend samples were sandwiched between two glass slides. The assembly was heated to 100 °C for 3 min to erase the thermal history, and then rapidly transferred into the hot stage set at the desired crystallization temperatures to allow the crystallization toward completion. To measure the melting temperatures (T'_ms) of the blends, the thermal crystallized samples were melt at a heating rate of 5 °C/min and the T'_ms were taken as the temperatures at which the crystals were totally molten.

Fourier transform infrared spectroscopy (*FTIR*). FTIR measurements were performed on a Bruker Equnox 55 Fourier transform infrared spectrometer equipped with a Specac variable temperature cell. The curing blends were granulated and the powder of blends were mixed with KBr and then pressed into small flakes for FTIR measurement. To investigate the intermolecular interactions at the elevated temperatures, the variable temperature measurement was carried out and the specimens were prepared by casting the dichloromethane solution of bisphenol A/PEO mixture (5% v/v) onto KBr windows. All the specimens used in the study were sufficiently thin to be within a range where the Beer–Lambert law is obeyed. The spectra were obtained at the resolution of 2 cm^{-1} and were averages of 64 scans.

Scanning electronic microscopy. The samples of the PBA-a/PEO blends were fractured under cryogenic conditions using liquid nitrogen. The fractured surfaces so obtained were immersed in chloroform at room temperature for 30 min. The PEO phase can be preferentially rinsed by the solvent while PBA-a phase remains unaffected. The etched specimens were dried to remove the solvents. All specimens were examined with a Hitachi S-2150 scanning electron microscope (SEM) at an activation voltage of 20 kV. The fracture surfaces were coated with thin layers of gold of about 100 Å.

3. Results and discussion

3.1. Miscibility in blends of BA-a and PEO

The miscibility of BA-a with PEO is essential to carry out the in situ polymerization of BA-a in the presence of PEO. All the BA-a/PEO blends with PEO content less than 40 wt% were transparent at ambient temperature. The blends with PEO >50 wt% were opaque at room temperature due to the crystallization of PEO in the mixtures, which was evidenced by the observation of spherulites using POM. Heated up to 80 °C, the opaque samples became transparent and the clarity can be reserved until 180 °C for ca. 40 min. The clarity suggests that the BA-a/PEO blends are miscible in the molten state, i.e. no phase separation occurred at the scale less than the wavelength of visible lights. All the BA-a/PEO blends were subjected to thermal analysis and the DSC curves are shown in Fig. 1. It can be seen that each blend displayed a single glass transition temperature (T_g), intermediate between those of the two pure components and varying with the blend composition. The conclusion is thus reached that the BA-a/PEO blends are completely miscible in the amorphous state. The miscibility of the BA-a/PEO blends is attributed to the non-negligible entropy contribution to free energy of mixing as the molecular weight of BA-a is rather low. From Fig. 1, it is also seen that no cold crystallization exothermic transition was observed in the DSC curves of pure PEO, 10:90, 20:80, 30:70 BA-a/PEO blends since crystallization was sufficiently rapid and occurred to completion during the quenching. The DSC curves of 40:60, 50:50 and 60:40 BA-a/PEO blends displayed crystallization transition during heating scan, implying that the crystallization of PEO becomes progressively difficult in BA-a-rich blends. While BA-a content is 70 wt%, the blends did not show any crystallinity. This is characteristic of a miscible blend system composed of a crystalline polymer and an amorphous component, which possesses the higher T_g.

It is seen that from Fig. 1, the melting temperature (T_m) of PEO in the blends significantly decreased with addition of BA-a to the system. The equilibrium melting points (T^0_m) were determined by Hoffman–Weeks analysis [47,48] and summarized in Table 1. In the BA-a/PEO blends, the equilibrium melting point depression is due mainly to the thermodynamic effects of mixing in the miscible crystalline polymer (PEO)-diluent (BA-a) system. From the values of

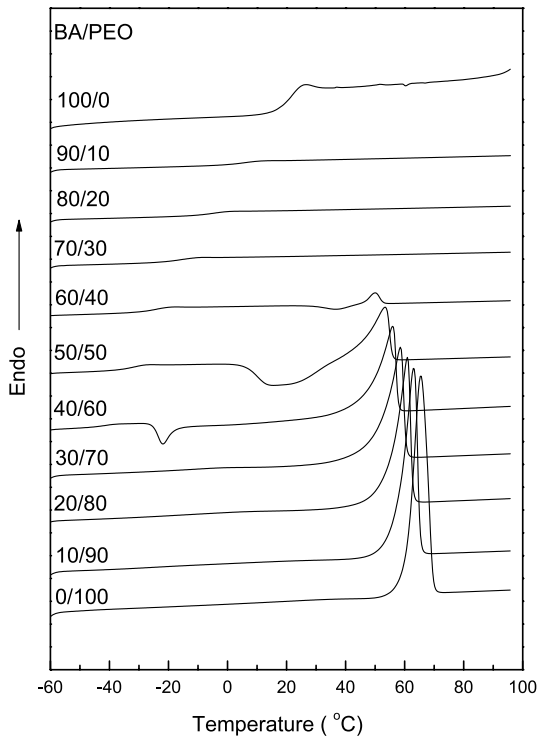

Fig. 1. DSC curves of BA-a/PEO blends (the second scans after quenching from 100 °C).

Table 1
Equilibrium melting points for BA-a/PEO blends

BA-a/PEO (wt)	Equilibrium melting point (°C)
0:100	71.1
10:90	68.1
20:80	67.0
30:70	65.9
40:60	64.8

equilibrium melting points, the intermolecular interaction parameter, χ_{12} can be estimated according to Scott theory, which was modified and given [49,50]:

$$\frac{1}{T_m^{0\prime}} - \frac{1}{T_m^0} = -\frac{RV_{2u}}{\Delta H_{2u} V_{1u}} \times \left[\frac{\ln(1-\phi_1)}{m_2} - \left(\frac{1}{m_2} - \frac{1}{m_1}\right)\phi_1 + \chi_{12}\phi_1^2 \right] \quad (1)$$

where the subscripts 1 and 2 denote the amorphous and crystalline components, respectively. ϕ is the volume fraction, V_u is the molar volume of the repeating unit, ΔH_{2u} refers to the fusion enthalpy per mole of 100% crystalline PEO. $T_m^{0\prime}$ and T_m^0 are the equilibrium melting points of the blends and the pure crystalline component. R is the universal gas constant and m is essentially the degree of polymerization. Eq. (1) can be rearranged into the following form:

$$\frac{\Delta H_{2u} V_{1u}}{RV_{2u}}\left[\frac{1}{T_m^{0\prime}} - \frac{1}{T_m^0}\right] + \frac{\ln(1-\phi_1)}{m_2} + \left(\frac{1}{m_2} - \frac{1}{m_1}\right)\phi_1 = -\frac{BV_{1u}}{R}\frac{\phi_1^2}{T_m^{0\prime}} \quad (2)$$

where B is the interaction energy density. The interaction parameter χ_{12} can be written as:

$$\chi_{12} = \frac{BV_{1u}}{RT} \quad (3)$$

In this work, several constants were taken as $\Delta H_{2u} = 205$ J/g [40] and $V_{1u} = 426.4$ cm^3/mol and $V_{2u} = 38.9$ cm^3/mol. Owing to the small molecular weight of BA-a, enthalpic and entropic effects all contribute the melting point depression. Therefore, interaction density, B and consequently χ_{12} were directly evaluated by plotting the left terms of Eq. (2) vs. φ_1^2/T_m^0 as shown in Fig. 2. From the slope, B and consequently χ_{12} were obtained to be $-.72$ cal/cm^3 and $-.45$ at 344 K, and the negative value of B suggests that the BA-a/PEO blends are miscible in the melt state.

Fig. 3 shows the crystallinity of PEO, as a function of blend composition, which was calculated from the

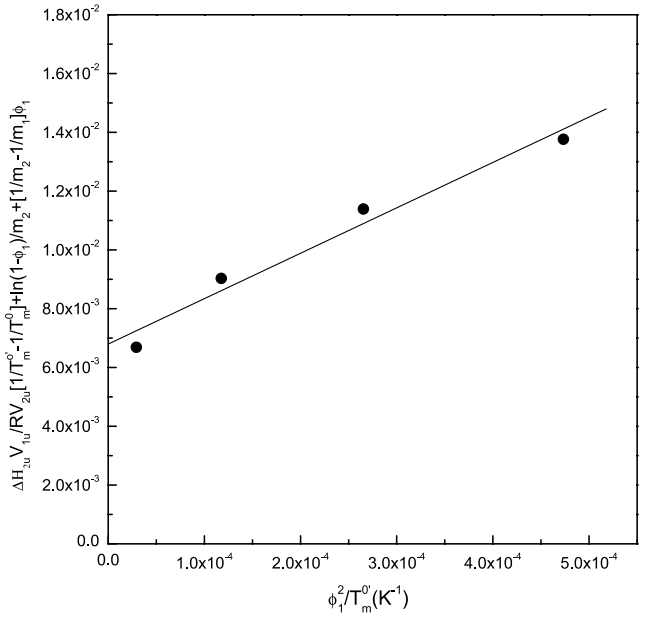

Fig. 2. Determination of intermolecular interaction parameters, B and χ_{12} for BA-a/PEO blends.

following equation:

$$X_c = (\Delta H_f - \Delta H_c)/\Delta H_f^0 \quad (4)$$

Where X_c is percent crystallinity. ΔH_f and ΔH_c are the enthalpy of fusion and crystallization of PEO, respectively. ΔH_f^0 is the fusion enthalpy of perfectly crystallized PEO, and it has been reported to be 205 J/g [40]. The crystallinity of PEO in the blends containing BA-a less than 30 wt% did not deviate much from the dashed

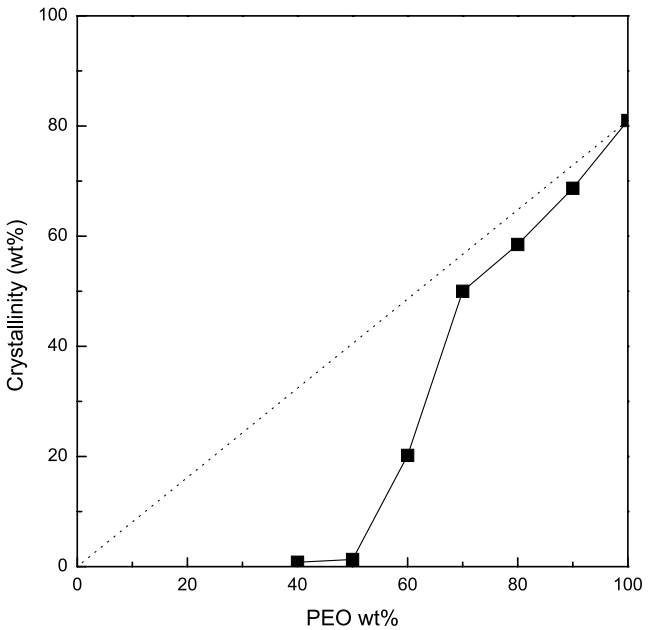

Fig. 3. The plot of percent crystallinity of PEO as a function of PEO concentration in BA-a/PEO blends. The dash line stands for the crystallinity of PEO blends with BA-a if the crystallization process were not influenced by the non-crystallizable components.

line, which stands for the crystallinity in the blends if the crystallization process were not influenced by the presence of BA-a and thus suffices the additivity. It is seen that there is a dramatic decrease in crystallinity when the content of BA-a is more than 20 wt%, indicating a pronounced inhibition of crystallization by the presence of BA-a.

Shown in Fig. 4 are the plots of thermal transition of the blends as a function of weight fraction of PEO. The T_g-composition relationship was accounted for by Gordon–Taylor equation [41]:

$$T_g = T_{g1} + k(W_2/W_1)\,(T_{g2} - T_g) \quad (5)$$

where T_g is the glass transition temperature of the blends, and the T_{g1} and T_{g2} are those of the blend components. W_i is the weight fraction. The k is an adjusting parameter related to the degree of curvature of the T_g-composition curve. It has been proposed that k can be taken as a semi-quantitative measure of miscibility and strength of the intermolecular interaction between components of polymer blends [3,42,43]. For instance, in the blends of PCL with chlorinated polyethylene, poly(vinyl chloride) and chlorinated poly(vinyl chloride), the k values increases from 0.26 to 1.0 with increasing the degree of chlorination, which gives rise to the increase in the amount of the intermolecular hydrogen-bonding between α-H of the chlorinated polymers and carbonyl of PCL. The application of Gordon–Taylor equation to the experimental data yielded a k value of 0.55, fitting the experimental data quite well. It should be pointed out that in the fitting the T_g values of PEO-rich blends (with PEO more than 70 wt%) were not used since there is the compositional enrichment of the amorphous region created by crystallization of PEO [44–46]. It was noted that the T_g of blends with PEO more than 70 wt% displayed the obvious positive deviation from the prediction by Gordon–Taylor equation. From Fig. 4, it is seen that the melting temperatures (T_m) of PEO decreased, characteristic of miscible polymer blends. The crystallization temperatures (T_c) of PEO in the blends increased with increasing BA-a concentration, indicating the inhabitation effect of the amorphous component on crystallization in the miscible blends.

3.2. Phase separation in blends of PBA-a and PEO

Differential scanning calorimetry. The BA-a/PEO blends were cured at elevated temperature and the mixtures of BA-a and PEO were thus converted into the thermosetting binary blends, i.e. in situ formed blends of PBA-a and PEO. The PBA-a/PEO with PEO content up to 90 wt% were prepared. It was observed that all the initially transparent mixtures of BA-a/PEO gradually became cloudy as the curing reaction proceeded within 40 min, suggesting the occurrence of phase separation induced by polymerization. The PBA-a/PEO blends were subjected to thermal analysis and the DSC curves are shown in Fig. 5. Ishida et al. [29] reported that the control PBA-a displayed a glass transition temperature (T_g) of ca. 163 °C although in the DSC thermograms the magnitude of this transition is quite small due possibly to a high crosslinking level, which restricts segmental motion. In a marked contrast to that in the uncured BA-a/PEO blends, the DSC thermograms of all

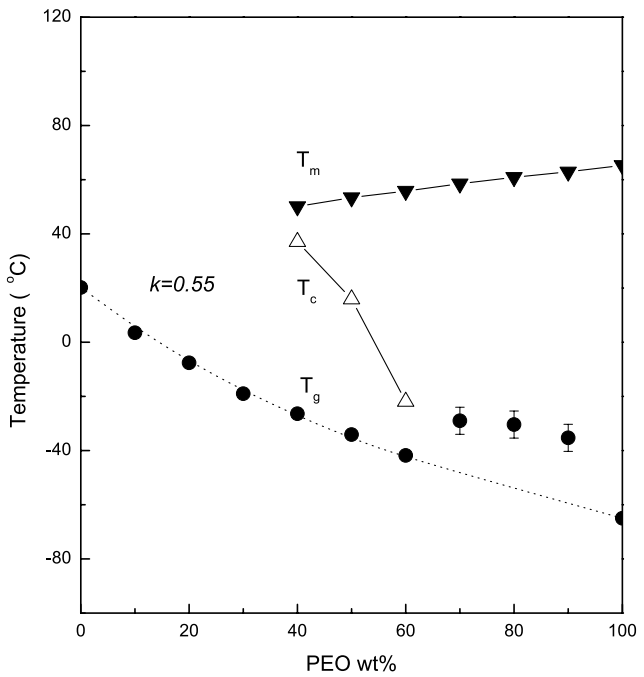

Fig. 4. Thermal transition of PBA-a/PEO blends. The dash line is drawn from the application of Gordon–Taylor equation with $k = 0.55$.

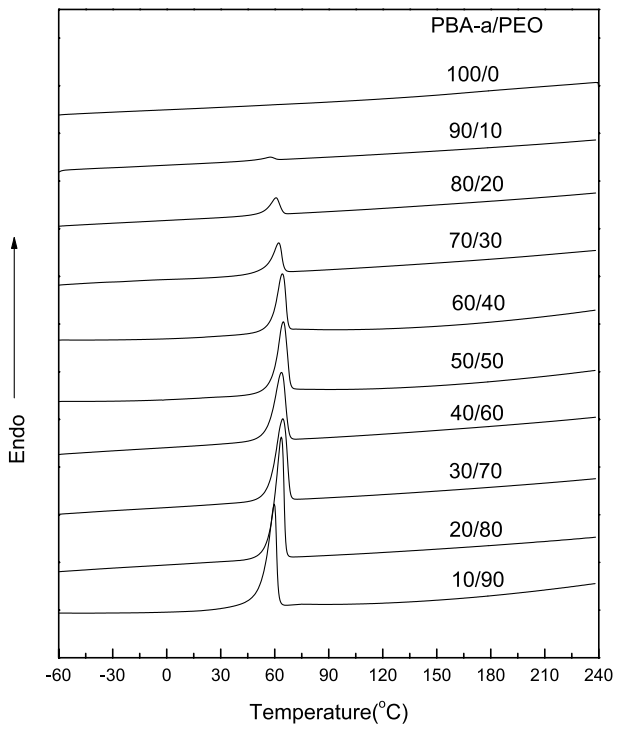

Fig. 5. DSC curves of PBA-a/PEO blends (the second scans after quenching from 180 °C).

the quenched cured blends displayed no evidence of crystallization during the heating scans, and instead showed the single endothermic peaks almost at constant temperature, corresponding to the fusion of PEO. Calorimetric analysis has been used to investigate miscibility of polymer blends by observing single glass transition temperatures intermediate between those of pure components, whereas the appearance of two T_g's indicates the occurrence of phase separation. However, for the polymer blends containing both a highly-crosslinked thermosetting component and a crystalline polymer, it becomes difficult unambiguously to identify phase separation by following the appearance of two glass transition temperatures because the magnitudes of glass transition are quite weak due to the high level of crosslinking and crystallinity. Nevertheless, the changes of other properties of blends, such as crystallinity can alternatively provide the information on phase separation, which have been used as the probes of phase separation [51, 52]. Shown in Fig. 6 is a plot of crystallinity as a function of blend composition for the PBA-a/PEO blends. It is seen that the crystallinity of PEO in the blends is almost coincident with the dashed line, which was drawn if the crystallization of PEO were not influenced by the presence of PBA-a, i.e. the crystallinity thus suffices the additivity with respect of blend composition. This result indicates the occurrence of the phase separation induced by polymerization occurred in the PBA-a/PEO blends. The phase-separated nature of the cured blends could be responsible for the higher crystallization capability to PEO, comparable to that of pure PEO. In the cured blends, PEO separates out during curing and thus it is easier for PEO to crystallize from the PEO-rich phase than from a miscible BA-a/PEO blends. It should be pointed out that the crystallinity of PBA-a/PEO 10:90 and 90:10 blends negatively deviated from the dashed line, suggesting that the blend at this composition could be partially miscible.

To observe the process of phase separation, the evolution of DSC thermograms with the curing time of the PBA-a/PEO 50:50 blend was representatively shown in Fig. 7. For the uncured BA-a/PEO 50:50 blends, the homogeneous and amorphous mixture was obtained after quenching from 100 to −0 °C since the enthalpic values of the crystallization and melting peaks are almost equal, suggesting that PEO crystallizes only during the heating run of DSC after quenching. The DSC curve of the blend cured for 20 min showed that the fusion enthalpy began to increase and even surpass that of crystallization, suggesting the PEO in the blend crystallized not only during the heating scan but also during the quenching process. At the same time, the melting temperatures (T_m) were observed to shift to the higher temperature. The shift of the melting transition to the higher temperature indicates that composition might have somewhat changed, implying the relative homogeneity in composition, i.e. both the components become partially miscible. In other words, two amorphous phases could form, i.e. one is PBA-a-rich phase, in which PBA-a is highly branched or slightly crosslinked, whereas another one corresponds to PEO-rich phase. In the PEO-rich phase, PEO chain can crystallize during quenching as in the uncured BA-a/PEO 30:70 blend (see Fig. 1). In this phase, the cold crystallization of PEO becomes easier, i.e. the hindrance effect of the amorphous component on PEO crystallization is decreased since a part of amorphous

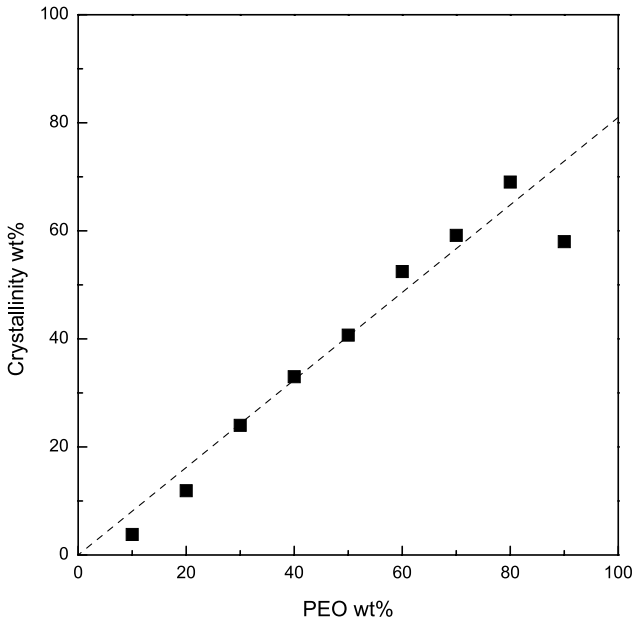

Fig. 6. The plot of percent crystallinity of PEO in PBA-a/PEO blends. The dash line stands for the crystallinity of PEO blends with PBA-a if the crystallization process were not influenced by the non-crystallizable components.

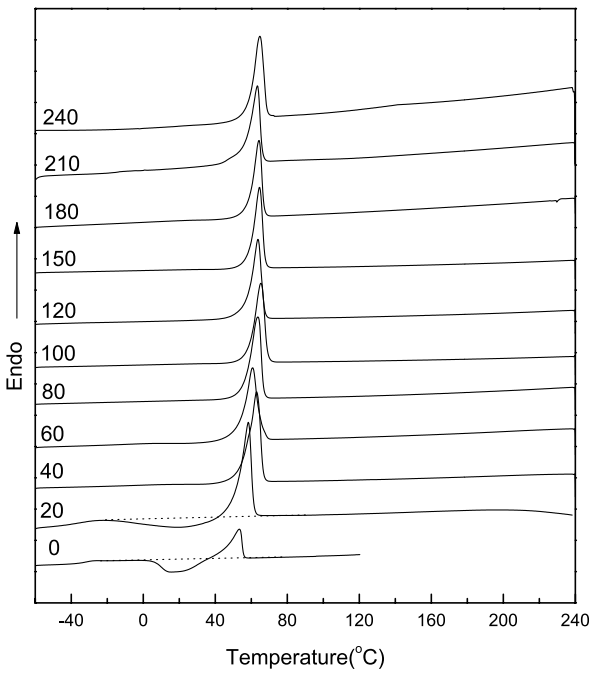

Fig. 7. DSC curves of BA-a/PEO 50:50 (wt) blends cured at various curing time.

component (PBA-a) with the higher T_g was to some extent separated out. As a consequence, the enthalpy of fusion increased, and T_m increased because of the formation of more perfect crystals. With curing proceeding, the crosslinking degree increased and the glass transition temperature of amorphous component also increased. Therefore, the degree of supercooling (i.e. $T_m - T_g$) for crystallization is reduced and crystallization temperature (T_c) will occur at higher temperature. It should be pointed out that the flat transition at ca. 200 °C is responsible for the endothermic curing reaction. It is seen that after curing for 40 min, the DSC curves of the blends almost remained invariant with increasing curing time. All the DSC curves displayed the single peaks attributable for the melting transition of PEO in the PEO-rich phase, which behaves just as in pure PEO, indicating that the phase separation induced by crosslinking occurred to completion.

Scanning electronic microscopy. The morphology of the PBA-a/PEO blends were investigated by SEM. Fig. 8 presents SEM micrographs of chloroform-etched fracture surfaces of the blends, which were frozen by liquid nitrogen. The heterogeneous morphology was observed in all the cases, which was in a good agreement with the results of DSC, i.e. the blends were phase separated. For PBA-a/PEO 90:10 blend, it can be seen that the spherical particle was uniformly dispersed in the continuous matrix after PEO phase was rinsed by chloroform and the size of spherical particles is ca. 0.5 μm in diameter. The spherical phase was

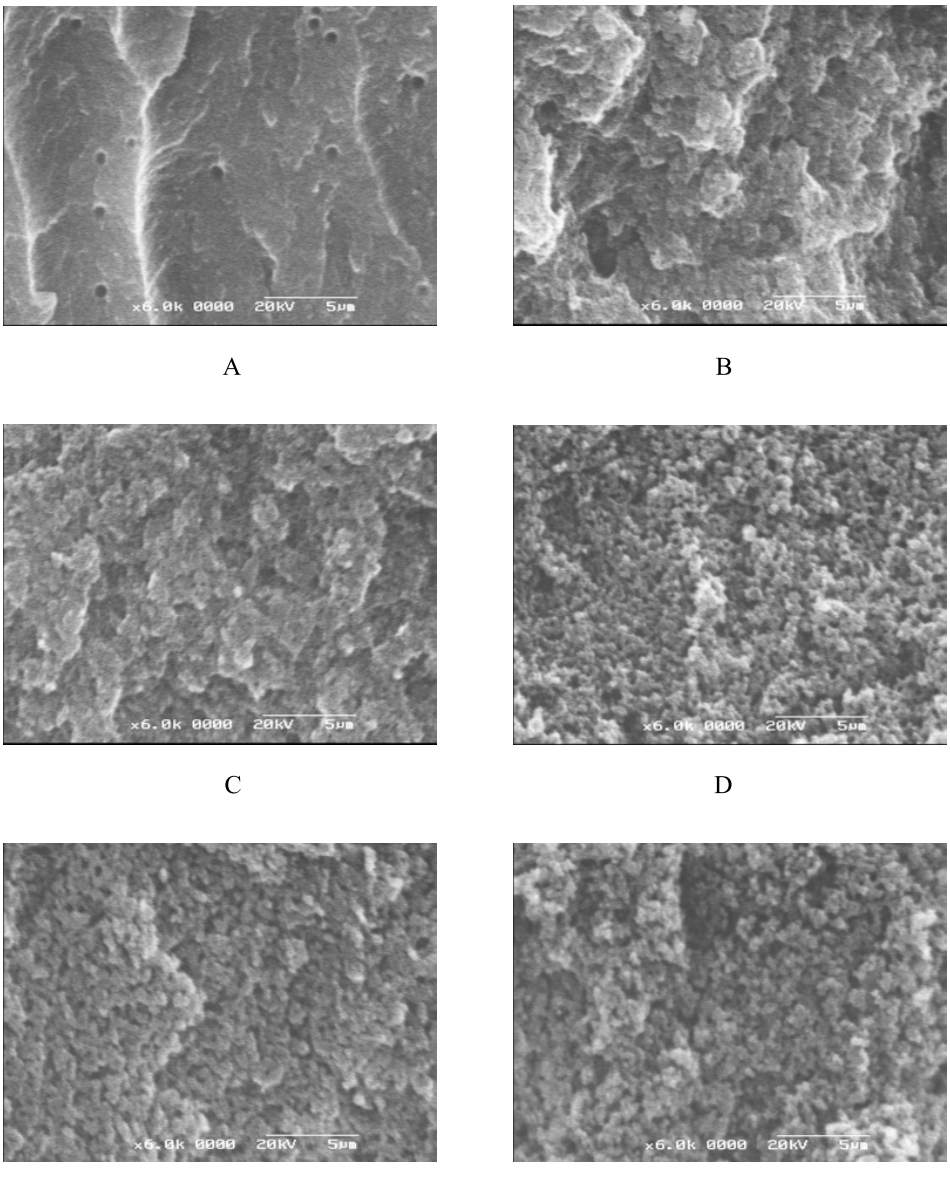

Fig. 8. SEM micrographs of PBA-a/PEO: (A) 90:10; (B) 80:20; (C) 70:30; (D) 60:40; (E) 50:50 and (F) 40:60.

attributed to PEO-rich phase whereas the continuous was ascribed to the PBA-a matrix. With increasing PEO, the blends displayed remarkably different morphologies (Fig. 8(B)–(F)). For PBA-a/PEO 80:20 blend, it is seen that PEO domains began to inter-connect and exhibited irregular shapes. At the same time, there appear the spherical particles on the surface of the etched blends with broad distribution of size, which are responsible for PBA-a phase since PEO-rich phase was dissolved by chloroform. Therefore, this is a combined morphology, i.e. the phase inversion began to appear; the totally phase-inverted morphology was observed for blends with PEO content more than 30 wt%. The average size of spherical PBA-a particle slightly decreased with increasing PEO content. Similar observations can be found in some thermoplastics-modified epoxy systems [53–57]. For thermoplastics-modified epoxy systems, the size of epoxy particles decreases with increasing thermoplastics concentration, which was attributed to the deceleration of phase separation and coarsening as well as incomplete curing reaction due to the inclusion of thermoplastics of high viscosity [53].

Interpretation of phase behavior. In hydrogen-bonded polymer blends, the free energy of mixing may be expressed by the following equation [35,36]:

$$\frac{\Delta G_{\mathrm{m}}}{RT} = \left(\frac{\Phi_{\mathrm{A}}}{N_{\mathrm{A}}}\ln \Phi_{\mathrm{A}} + \frac{\Phi_{\mathrm{B}}}{N_{\mathrm{B}}}\ln \Phi_{\mathrm{B}}\right) + \chi \Phi_A \Phi_B + \frac{\Delta G_H}{RT} \quad (6)$$

Where Φ_{A} and Φ_{B}, and N_{A} and N_{B}, are the volume fractions and degrees of polymerization of polymers A and B, respectively. The first two bracketed terms are from the contribution of combinatorial entropy. χ is a conventional Flory–Huggins interaction parameter, which can be evaluated by using the non-hydrogen-bonded solubility parameters according to the Scatchard–Hildebrand relation. The last term is denoted by $\Delta G_{\mathrm{H}}/RT$, and is the contribution of hydrogen bonding interaction to mixing. For high molecular mass polymers (e.g. crosslinked polymers), the contribution from combinatorial entropy is negligibly small and the χ term always embodies the unfavorable physical interaction against mixing. Therefore, the last term ($\Delta G_{\mathrm{H}}/RT$) is crucial to the miscibility of polymer blends. In fact, the most of polymer blends found hitherto are immiscible unless there exist the favorable intermolecular specific interactions (e.g. hydrogen bonding); the intermolecular specific interactions have been taken as the driving force for miscibility in thermosetting polymer blends [21–23].

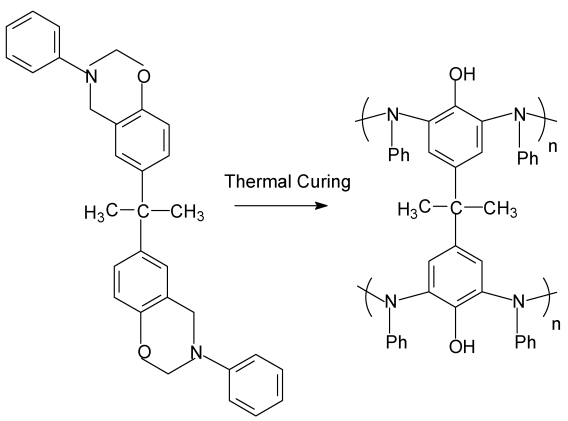

Scheme 2.

In the present case, the thermal curing of BA-a resin will afford a great number of phenolic hydroxyls (see Scheme 2) in the crosslinked backbone of PBA-a, which are potential to form the intermolecular hydrogen bonding interactions with ether oxygen atoms of PEO and thus fulfill the miscibility of PBA-a with PEO. However, both DSC and SEM investigations indicate that the blends were phase-separated, implying that there could not be the favorable intermolecular hydrogen bonds in the system in the curing condition. To confirm the speculation, it is necessary to examine the intermolecular specific interactions at the curing temperature. Nonetheless, an appropriate model compound for PBA-a should be selected. Herewith, bisphenol A is used and PBA-a can be taken as the substituted (or crosslinked) bisphenol A. Fig. 9 presents a series of FTIR spectra of bisphenol A/PEO 50:50 blend, which were recorded at various temperatures. Bisphenol A was characteristic of the stretching vibration of phenolic hydroxyl at 3349 cm^{-1} (curve A) and the broad band was attributed to self-associated hydroxyls and the width of the

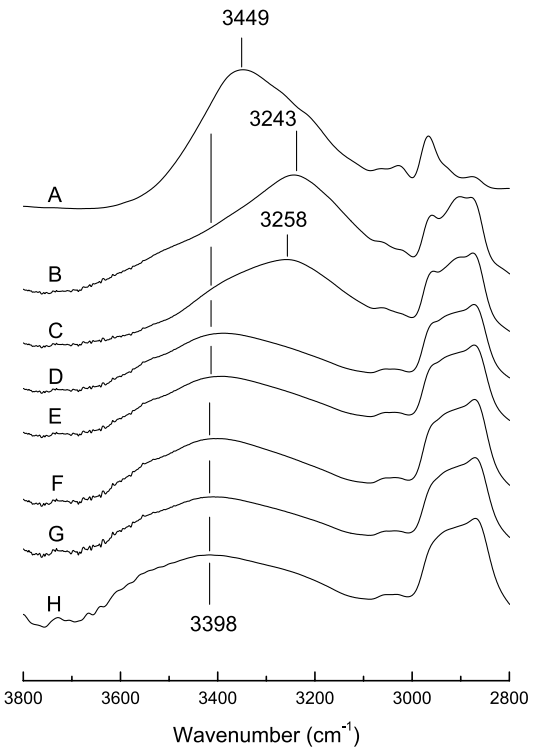

Fig. 9. Variable temperature FTIR spectra of bisphenol A/PEO 50:50 blend in the range of 2800–3800 cm^{-1}. (A) Pure bisphenol A at room temperature; (B) bisphenol A/PEO 50:50 blend at room temperature; (C) the blend at 100 °C; (D) the blend at 160 °C; (E) the blend at 170 °C; (F) the blend at 180 °C; (G) the blend at 190 °C and (H) the blend at 200 °C.

band reflects the wide distribution of hydrogen-bonded hydroxyl stretching frequencies. Upon mixing PEO to system, the hydroxyl bands are observed to shift to a lower frequency (3243 cm^{-1}) when PEO concentration is 50 wt% (see curve B), suggesting the formation of the intermolecular hydrogen bonding interactions between bisphenol A and PEO, and that the intermolecular hydrogen bonding strength is much stronger than that self-association of pure bisphenol A. When heated this sample up to 80 °C, the hydroxyl stretching vibration band is observed to shift to the higher frequency at 3258 cm^{-1}, implying that the strength of the intermolecular hydrogen bonding was reduced at the elevated temperature. At the same time, there newly appears a shoulder band at 3398 cm^{-1}, which was ascribed to the stretching vibration of the free phenolic hydroxyls. When the sample was heated up to 160 °C or higher temperatures, the intermolecular hydrogen bonded hydroxyl bands disappeared, and instead the strength of the free hydroxyl bands increased (see curves D to H), suggesting that the phenolic hydroxyls existed in the blend system in the non-associated (or free) form, i.e. the intermolecular hydrogen bonding interactions were significantly eliminated. The observation is important to help to understand the phase behavior of PBA-a/PEO blends. At the elevated temperatures (e.g. the curing temperature), the miscibility of the components is mainly governed by the combinatory entropic contribution in Eq. (6), other than the $\Delta G_H/RT$ term. With the curing reaction proceeding at elevated temperatures, a serial of structural changes involving chain extension, branching and crosslinking occurred in succession and the molecular weight of system greatly increased and three-dimensional networks were formed. The increased molecular weight gives rise to the decrease of entropy contribution to miscibility. Therefore, the phase separation induced by polymerization occurred. In comparison with the pure PBA-a, there is only the small frequency shift of hydroxyl stretching vibration bands for PBA-a/PEO 70:30, 50:50 and 30:70 blends as shown in Fig. 10, indicating that the phase separation is quite complete in these blends. For PBA-a/PEO 90:10 blend, there are two components in the FTIR spectrum of hydroxyl stretching vibration range. The one of them is centered at 3443 cm^{-1} and the other bands appeared at the lower frequency (3363 cm^{-1}). The bands at the lower frequency could be responsible for the hydrogen-bonded hydroxyls of PBA-a with ether oxygen atoms of PEO. For PBA-a/PEO 10:90 blend, the hydroxyl bands were observed to shift to the lower frequency by 13 cm^{-1}. The above observation indicates that the strength of hydrogen bonding between PBA-a and PEO is stronger than that of the self-association of PBA-a if the intermolecular hydrogen bonding interactions are allowed to form. The feature of FTIR spectra for 90:10 and 10:90 PBA-a/PEO blends was in a good agreement with the results of DSC, i.e. the blends at the compositions are partially miscible.

It should be pointed out that the intermolecular hydrogen bonding interactions in the mixture of bisphenol A and PEO does not exactly represent the case in PBA-a/PEO blends although PBA-a can be taken as substituted bisphenol A. In fact, the occurrence of crosslinking (or substitution) could weaken the intermolecular hydrogen bonding interactions. Coleman et al.. [58,59] have observed that the intramolecular and intermolecular hydrogen bonding interactions were significantly reduced by increasing the size of the substituted groups due to the steric hindrance in the blends of 2,6-dialkyl substituted poly(4-vinyl phenol)s. In the present system, it is proposed that the formation of the three-dimensional crosslinking network could reduce the intramolecular and intermolecular hydrogen bonding interactions among phenolic hydroxyls and phenolic hydroxyl vs. ether oxygen atom of PEO if there exit the H-bonding interactions. In addition, the changes of intermolecular hydrogen bonding interaction in the screening effect and chain connectivity resulting from crosslinking should also be implicated [38,60].

4. Conclusions

Thermosetting blends composed of PBA-a and PEO were prepared via in situ curing reaction of BA-a in the presence of PEO, which started from the initially homogeneous mixtures of BA-a and PEO. Before curing, the single and composition-dependant glass transition temperatures (T_g's) were observed in the entire blend composition for BA-a/PEO blends. The experimental T_g's were well predicted by Gordon–Taylor equation. The equilibrium

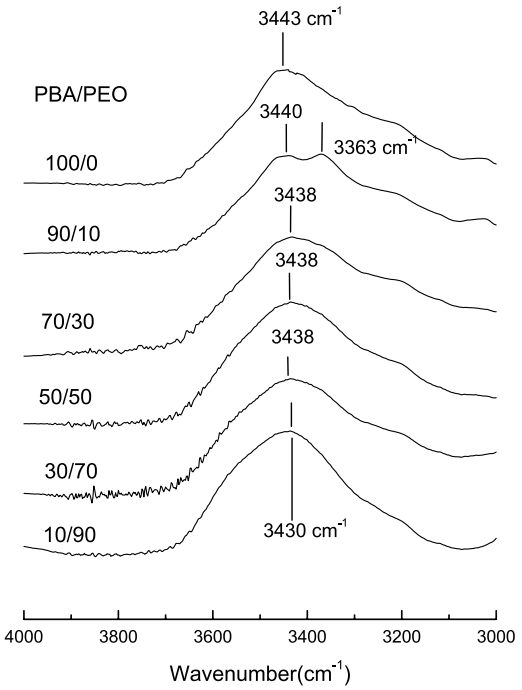

Fig. 10. The FTIR spectra of the as-prepared PBA-a/PEO blends in the range of 3000–4000 cm^{-1}, recorded at the ambient temperature.

melting point depression is observed for the uncured BA-a/PEO blends. The miscibility of the blends was mainly ascribed to the contribution of entropy to mixing free energy since the molecular weight of BA-a is rather low. However, phase separation occurred after curing reaction, which was confirmed by DSC and SEM. It was expected that the PBA-a/PEO blends would be miscible since there are a great number of phenolic hydroxyls formed during the curing reaction, which are potential to hydrogen bonding with oxygen atoms of PEO and thus would fulfill the miscibility of the blends via the specific intermolecular interaction. However, our investigation by means of variable temperature FTIR via model compounds indicates that the phenolic hydroxyl groups could not form the favorable intermolecular hydrogen bonding interactions at the elevated temperatures (e.g. the curing temperatures), i.e. the phenolic hydroxyl groups existed mainly in the non-associated form in the system. Therefore, the phase separation is still ascribed to the decrease of the entropic contribution to mixing energy due to the increase of molecular weight.

Acknowledgements

This work is financially supported by the Excellent Young Teachers Program (EYTP, Project No. 2066) of Ministry of Education, P. R. China. The partial support from Shanghai Science and Technology Commission, China under a key project (No. 02DJ14048) was acknowledged.

References

[1] Paul DR, Newman S, editors. Polymer blends, vols. 1–2. New York: Academic Press; 1978.
[2] Olabisi O, Robeson LM, Shaw MT. Polymer–polymer miscibility. New York: Academic Press; 1979.
[3] Utracki LA. Polymer alloys and blends: thermodynamics and rheology. Munich: Hanser; 1989. p. 94.
[4] Noshay A, Robeson LM. J Polym Sci Part A: Polym Chem 1974;12: 689.
[5] Clark JN, Daly JH, Garton A. J Appl Polym Sci 1984;29:3381.
[6] Guo Q, Peng X, Wang Z. Polymer 1991;32:53.
[7] Luo X, Zheng S, Zhang N, Ma D. Polymer 1994;35:2619.
[8] Zheng S, Zhang N, Luo X, Ma D. Polymer 1995;36:3609.
[9] Zheng H, Zheng S, Guo Q. J Polym Sci Part A: Polym Chem 1997;35: 3161.
[10] Zheng H, Zheng S, Guo Q. J Polym Sci Part A: Polym Chem 1997;35: 3169.
[11] Zheng S, Zheng H, Guo Q. J Polym Sci Part B: Polym Phys 2003;41: 1085.
[12] Zheng S, Lü H, Chen C, Nie K, Guo Q. Colloid Polym Sci. published online May 2003.
[13] Oyanguren PA, Frontini PM, Williams RJJ, Girard-Reydet E, Pascault JP. Polymer 1996;37:3079.
[14] Oyanguren PA, Frontini PM, Williams RJJ, Vigier G, Pascault JP. Polymer 1996;37:3087.
[15] Mijovic J, Shen M, Sy JW, Mondragon I. Macromolecules 2000;33: 5235.
[16] Guo Q, Thomann R, Gronski W, Thurn-Albrecht T. Macromolecules 2002;35:3133.
[17] Guo Q, Zheng H. Polymer 1999;40:637.
[18] Guo Q, Zheng H. J Appl Polym Sci 1999;74:332.
[19] Chen J-L, Chang F-C. Macromolecules 1999;32:5348.
[20] Remiro PM, Cortazar MM, Calahorra ME, Calafel MM. Macromol Chem Phys 2001;202:1077.
[21] Guo Q, Harrats C, Groeninckx G, Koch MHJ. Polymer 2001;42:4127.
[22] Guo Q, Harrats C, Groeninckx G, Reynaers H, Koch MHJ. Polymer 2001;42:6031.
[23] Guo Q, Groeninckx G. Polymer 2001;42:8647.
[24] Teng K-C, Chang F-C. Polymer 1996;37:2385.
[25] Ning X, Ishida H. J Polym Sci, Part A: Polym Chem 1994;32:1121.
[26] Shen SB, Ishida H. J Appl Polym Sci 1996;61:1595.
[27] Kim HJ, Zdenka B, Ishida H. Polymer 1999;40:1815.
[28] Ishida H, Lee Y-H. Polymer 2001;42:6971.
[29] Ishida H, Lee Y-H. J Polym Sci, Part B: Polym Phys 2001;39:736.
[30] Takeichi T, Agag T, Zeidam R. J Polym Sci, Part A: Polym Chem 2001;39:2633.
[31] Coleman MM, Pehlert GJ, Painter PC. Macromolecules 1996;29: 6820.
[32] Pehlert GJ, Painter PC, Veytsman B, Coleman MM. Macromolecules 1997;31:8423.
[33] Pehlert GJ, Painter PC, Coleman MM. Macromolecules 1998;31: 8423.
[34] Pruthtikul R, Coleman MM, Painter PC. Macromolecules 2001;34: 4145.
[35] Coleman MM, Graf JF, Painter PC. Specific interactions and the miscibility of polymer blends. Lancaster, PA: Technomic Publishing; 1991.
[36] Coleman MM, Painter PC. Prog Polym Sci 1995;20:1.
[37] Coleman MM, Painter PC. Macromol Chem Phys 1998;199:1307.
[38] Hu Y, Gamble V, Painter PC, Coleman MM. Macromolecules 2002; 35:1289.
[39] Ishida H, Allen DJ. J Polym Sci, Part B: Polym Phys 1996;34:1019.
[40] Vidotto G, Levy DL, Kovacs AJ. Kolloid Z Polym 1996;230:289.
[41] Gordon M, Taylor JS. J Appl Chem 1952;2:493.
[42] Belorgey G, Prud'homme RE. J Polym Sci, Part B: Polym Phys 1982; 20:191.
[43] Belorgey G, Aubin M, Prud'homme RE. Polymer 1982;23:1051.
[44] Li Y, Stein M, Jungnickel B-J. Colloid Polym Sci 1991;269:772.
[45] Li Y, Jungnickel B-J. Polymer 1993;34:9.
[46] Shibanov YD, Godovsky YK. Prog Colloid Polym Sci 1989;80:110.
[47] Hoffman JD, Weeks JJ. J Chem Phys 1962;37:1723.
[48] Hoffman JD, Weeks JJ. J Res Natl Bur Stand, Sect A 1962;66:13.
[49] Nishi T, Wang TT. Macromolecules 1975;8:909.
[50] Imken RL, Paul DR, Barlow JW. Polym Engng Sci 1976;16:593.
[51] Li W, Prud'homme RE. J Polym Sci, PartB: Polym Phys 1993;31:719.
[52] Zheng S, Huang J, Li Y, Guo Q. J Polym Sci, Part B: Polym Phys 1997;35:1383.
[53] Yamanaka K, Inoue T. Polymer 1989;30:662.
[54] Cho JB, Hwang JW, Cho K, An JH, Park CE. Polymer 1993;34:4832.
[55] Zheng S, Wang J, Guo Q, Wei J, Li J. Polymer 1996;37:4667.
[56] Zheng S, Hu Y, Guo Q, Wei J. Colloid Polym Sci 1996;274:410.
[57] Zheng S, Gao R, Li J, Guo Q. J Appl Polym Sci 2003;(89):505.
[58] Coleman MM, Pehlert GJ, Yang X, Stallman JB, Painter PC. Polymer 1996;37:4553.
[59] Pehlert GJ, Yang X, Painter PC, Coleman MM. Polymer 1996;37: 4763.
[60] Coleman MM, Hu Y, Sobkowiak M, Painter PC. J Polym Sci, Part B: Polym Phys 1998;36:1579.